ICEE 2026: 32nd International Council on Electrical Engineering Conference, July 5-9, 2026, KCCI, Seoul, Korea

Design and Analysis of Dual-Rotor Dual-Flux Switching Stator Permanent Magnet Motor

Zixu Dong*, Mingyuan Jiang†*, Zhang Zhang*, Zhouyang Zhang*, Shuangxia Niu*, K. T. Chau* and C. C. Chan*

Abstract – This paper proposes a novel dual-rotor dual flux-switching (DR-DFS) motor topology that leverages the synergistic advantages of both flux-switching and dual-rotor topologies. By simplifying the structural configuration and reducing permanent magnet (PM) consumption, the proposed design effectively mitigates manufacturing complexity and production costs, making it highly suitable for direct-drive applications. The electromagnetic performance, including torque output and back electromotive force, is comprehensively evaluated using the finite element method (FEM). Furthermore, a multi-objective optimization based on a genetic algorithm is implemented to refine the structural parameters and further maximize the output performance

Keywords: Dual-rotor, Flux modulation, Flux switching, PM, Torque ripple

1. Introduction

At present, the application of electrical energy is developing at an unprecedented speed, a trend that continues to advance with the continuous reduction of human society's dependence on fossil energy. Among the many fields driving this transformation, the rise of new energy industries such as electric vehicles [1],[2], hybrid vehicles [3][4], electric aircraft [5][6], wind power generation [7][8], and wave energy conversion [9][10]. Permanent magnet (PM) machines, such as the PM brushless machines [11][12], PM vernier machines [13][14], magnetic-geared machines [15][16], stator-PM machines [17][18] and flux-switching PM machines [19][20], occupy a pivotal position in the electric machine field by virtue of the outstanding advantages such as higher efficiency, higher reliability and higher torque density than the conventional DC machines [21], induction machines [22] and reluctance machines [23].

PM machines, which originated in the 19th century, are typically categorized as PM synchronous machines (PMSMs), also referred to as PM brushless AC motors (PMBLACMs). In the late 20th century, the rapid advancements in PM materials and power electronics propelled the development of PMSMs to a new height [24]. Conventional electric machines are typically characterized by a single-rotor configuration for mechanical power conversion. However, with the continuous advancement of engineering applications, conventional single-rotor topologies are increasingly struggling to meet evolving performance requirements. Consequently, dual-rotor machines (DRMs), which incorporate two rotors, have garnered significant attention in recent years. The flux modulation principle is extensively utilized in the design of DRMs and has increasingly permeated various engineering fields. In the field of wind power generation, this principle is employed to achieve flux-weakening control, thereby extending the operational speed range [25][26]. To enhance torque output in hybrid electric vehicles (HEVs) [27][28], and in EVs for direct-drive mode [29][30]. Additionally, this principle has been implemented in a wide range of other domains matched with DRMS to optimize overall system output performance [31]-[33]. However, to optimize flux paths and enhance flux density, conventional DRMs typically employ rotor-mounted PMs. This configuration poses a significant risk of PM detachment under high-speed operation due to centrifugal forces. Moreover, in DRMs featuring an internal rotor, the inherent challenges in heat dissipation can lead to excessive temperature rise, thereby increasing the risk of irreversible demagnetization [34].

Among various machine topologies, flux-switching PM machines (FSPMMs) represent a typical stator-PM architecture, which effectively circumvents the potential risks inherent in rotor PM designs [35]. FSPMMs are gaining attention in recent years since heat dissipation and reliability. To enhance the torque density of FSPMMs, a dual-PM configuration is adopted [36][37]. Furthermore, the fault-tolerant capability of the machine is significantly bolstered through optimized stator tooth geometries and the

† Corresponding Author: Dept. of Electrical and Electronic Engineering, The Hong Kong Polytechnic University, Hong Kong, China (m.y.jiang@polyu.edu.hk)

* Dept. of Electrical and Electronic Engineering, The Hong Kong Polytechnic University, Hong Kong, China (zixu06.dong@connect.polyu.hk)

implementation of advanced control strategies [38][39]. Significant research has been conducted on dual-rotor flux-switching (DRFS) machines, exploring their potential in direct-drive applications such as EVs and flywheel energy storage systems [40]-[42]. Despite their advantages, existing DRFS machines typically necessitate highly sophisticated stator and PM configurations. This structural intricacy increases the difficulty of precision fabrication and raises the overall production cost.

This paper proposes a novel dual-rotor dual-flux-switching PM (DR-DFS-PM) motor topology which is simple in design, easy to manufacture and has high robustness. This paper is structured into five sections. Following the introduction, the proposed topology and operating principles are detailed in Sections II and III, respectively. Section IV focuses on the performance analysis and structural optimization of the design, and the paper is concluded in Section V.

2. Proposed Motor Structure

Table 1. The basic parameters of proposed topology.

Items	Symbol	Value
Motor outer diameter	D_o	220mm
Motor active stack length	L_s	80mm
Air gap length	L_{air}	1mm
Stator slot number	Z	24
Inner rotor teeth number	N_{ki}	22
Outer rotor teeth number	N_{ko}	19
Winding I pole pair number	$P_{a,I}$	7
Winding II pole pair number	$P_{a,II}$	10

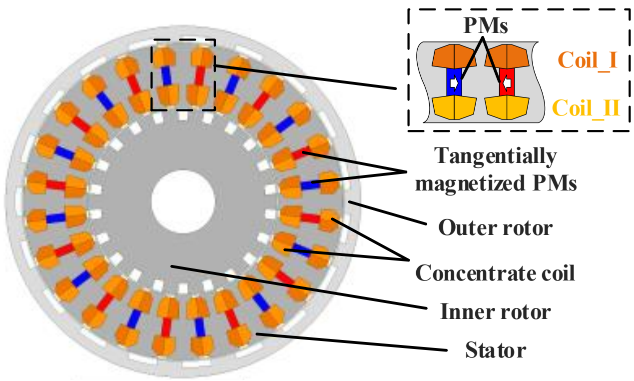

Fig. 1. The proposed DR-DFS-PM motor topology.

Fig. 1 illustrates the configuration of the proposed motor, which integrates a stator, an inner rotor, an outer rotor, and concentrated windings. All ferromagnetic elements in this design are constructed using DW310-35 silicon steel sheets. To amplify the magnetic flux capacity, tangentially magnetized PMs are embedded between inner stator slots and outer stator slots, working in synergy with the concentrated windings. Table 1 presents the basic parameters of the proposed topology. The stator is designed with 24 slots and is shared by both rotors. Both the inner and outer rotors utilize a conventional FS structure, featuring 22 and 19 teeth, respectively. Furthermore, the concentrated winding comprises two distinct sets dedicated to the inner and outer rotors, with their respective pole pair numbers specified as 7 and 10. The coordination between these pole pairs is governed by the following relationship:

$$P_r = \frac{Z}{2} \tag{1}$$

$$\begin{aligned} P_{a,I} &= |P_r - N_{ko}| = 7 \\ P_{a,II} &= |P_r - N_{ki}| = 10 \end{aligned} \tag{2}$$

where P_r is the stator PM pole pair number.

3. Operation Principle

3.1 Flux Circuit Analysis

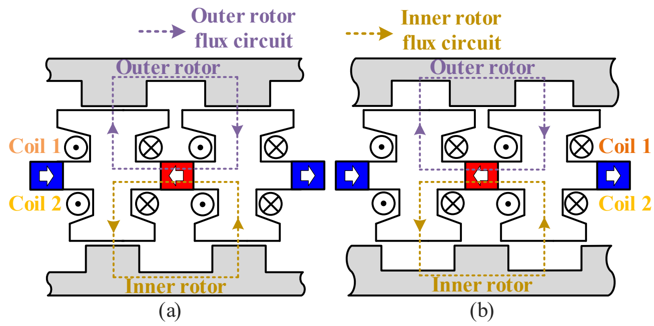

Fig. 2. The basic flux path of proposed DR-DFS-PM motor topology. (a) Aligned position. (b) Unaligned position.

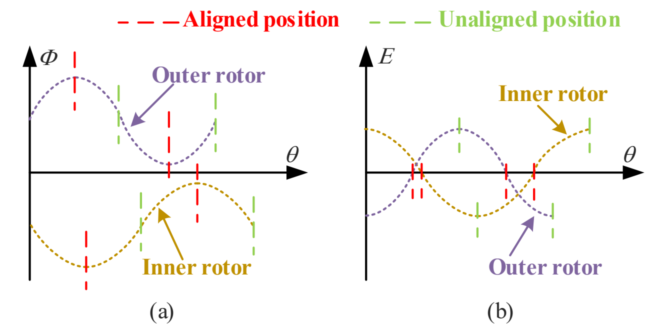

Fig. 3. Schematic coil flux and back EMF of proposed DR-DFS-PM motor topology. (a) Coil flux. (b) Back EMF.

Owing to the arrangement of tangentially magnetized PMs between the inner and outer stator slots, the proposed dual-FS structure exhibits a distinct flux-reversal effect during operation. Fig. 2 illustrates the magnetic flux paths within the inner and outer rotors. For analytical simplicity, the investigation focuses on two critical rotor positions: the aligned and unaligned positions relative to the stator teeth. In the aligned position, the magnetic circuit reaches its minimum reluctance, resulting in the maximum flux linkage.

Conversely, in the unaligned position, although the magnetic flux still forms a complete loop through the air gap, the reluctance is maximized, leading to a minimum flux linkage. Fig. 3 presents the periodic variations of flux linkage and the induced back electromotive force (back-EMF) under ideal operating conditions. Since the flux linkage alternates periodically with the rotor position, the induced back EMF likewise exhibits periodic characteristics. And the back-EMF reaches its maximum value at the unaligned position, the back-EMF is at the minimum at the aligned position. Moreover, the discrepancy in the tooth numbers of the inner and outer rotors leads to variations in their respective flux fluctuation periods and back EMF frequencies in the actual situation. Two other critical rotor positions are depicted in Fig. 4. In these configurations, the inner and outer rotors are situated in aligned and misaligned positions with respect to the stator poles. Consequently, the respective flux linkages attain their peak and trough values, while their magnetic directions are mutually reversed.

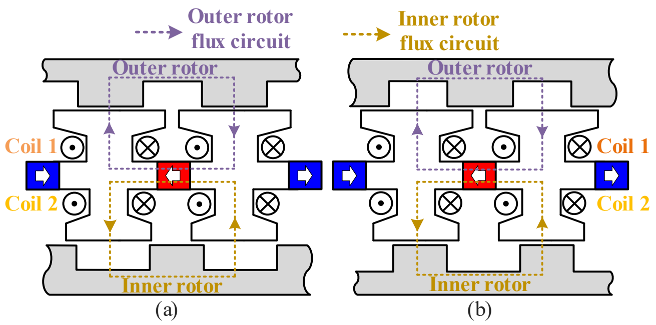

Fig. 4. The two rotors are respectively located at aligned position and unaligned position in actual operation.

3.2 Decoupling Analysis

In double-winding machine systems, achieving effective decoupling between the two sets of windings is a prerequisite for independent control and high-performance operation. Since both winding sets are integrated within a shared stator iron core which utilize the same magnetic circuit, leading to an inherent spatial overlap of their respective electromagnetic fields. This physical configuration inevitably introduces mutual inductance, where current transients in one winding set induce a parasitic back-EMF in the other, resulting in undesired cross-channel energy transfer and dynamic interference.

To analytically quantify this interaction, the mutual flux linkage $\Phi_{II,I}$, the flux linked by winding II due to the magnetic field of winding I, is expressed as follow [43]:

$$\Phi_{II,I} = L_s R_{air} \int_0^{2\pi} B_I(\theta) M_{II}(\theta) d\theta \tag{3}$$

where L_s is the stack length of the motor, R_{air} is the radius of air gap, $B_I(\theta)$ the resultant magnetic flux density distribution when winding I is excited without PM excitations, $M_{II}(\theta)$ is the winding function of winding II, which can be expressed as follow:

$$M_{II}(\theta) = \sum_{i=1,2,3\ldots} \frac{2Zk_{wi}}{i\pi P_{a,II}\cos(iP_{a,II}\theta)} \tag{4}$$

where k_{wi} is the winding factor of the i-th harmonic.

Through Fourier series expansion, it becomes evident that mutual flux linkage is only synthesized when both sets share common harmonic orders. Let H_I and H_{II} denote the sets of non-zero harmonic orders for the flux density and the winding function, respectively. The fundamental criterion for magnetic decoupling is established when $H_I \cap H_{II} = \emptyset$ [44]. Under this condition of harmonic orthogonality, the mutual inductance term vanishes. In addition, ensure that the distribution factor of winding I $(k_{d,I})$ relative to the harmonics of the winding II is minimized or nullified, thereby achieving a magnetically isolated dual-winding environment. Take the winding in this paper as an example,

$$\begin{aligned} H_I &= \{h \mid h = (2k-1)P_{a,I}\}, k \in Z^+ \\ H_{II} &= \{h \mid h = (2k-1)P_{a,II}\}, k \in Z^+ \end{aligned} \tag{5}$$

where $P_{a,I} = 7$ and $P_{a,II} = 10$, they are respectively an odd and an even, there can be no intersection between these two sets from a mathematical perspective, that is, $H_I \cap H_{II} = \emptyset$, which proves that these two sets of windings are decoupled.

4. FEM Simulation and Optimization

In this paper, the initial model was initially analyzed using finite element method (FEM) through the assistance of Maxwell based on the DR-DFS-PM motor topology designed based on Fig. 1.

4.1 No-load Analysis

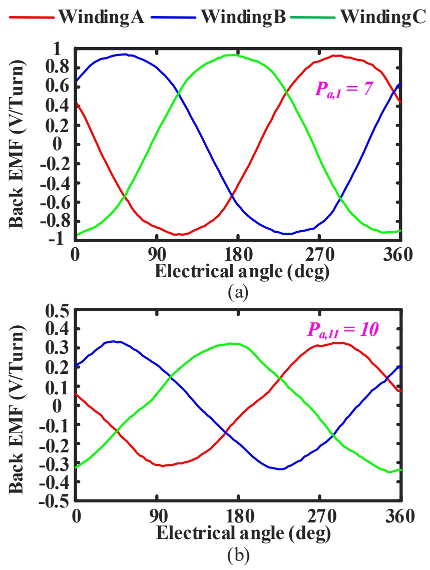

Fig. 5. The back EMF waveforms of the proposed DR-DFS-PM motor. (a) $P_{a,I} = 7$. (b) $P_{a,II} = 10$.

Fig. 5 depicts the back-EMF waveforms of both winding sets at a contra-rotating speed of 500 rpm. To eliminate the influence of slot area and fill factor on the performance evaluation, the back-EMF of a single-turn coil is analyzed. It is observed that winding I exhibits a more regular waveform compared to winding II. The single-turn amplitude of winding I is approximately 0.94 V, which is 185% higher than that of winding II.

Fig. 3 illustrates the magnetic flux distribution under no-load conditions. As depicted, the flux lines are uniformly distributed and align perfectly with the operation flux circuit analyzed previously.

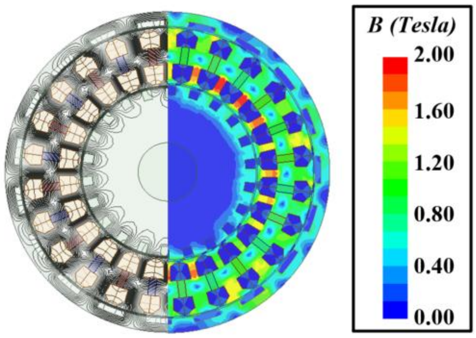

Fig. 6. The no-load flux line distribution and on-load flux density of the proposed motor.

4.2 Load Analysis

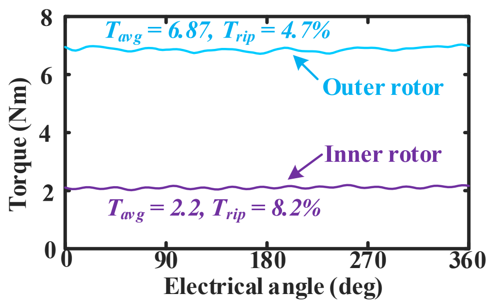

Fig. 7. The torque waveforms of inner rotor and outer rotor of the proposed motor.

Fig. 7 illustrates the torque waveforms of the inner and outer rotors over one electrical cycle. The average torque (T_{avg}) of the outer rotor is approximately triple that of the inner rotor, a disparity primarily attributed to the difference in rotor radius. Furthermore, the outer rotor exhibits a torque ripple (T_{rip}) of 4.7%, which is roughly half that of the inner rotor 8.7%. Notably, the T_{rip} of inner rotor remains within an acceptable range for practical applications.

Fig. 6 illustrates the magnetic flux density distribution under load conditions. While the overall magnetic circuit exhibits a well-managed saturation level, localized saturation is observed with peak flux densities reaching 2.0 T. This localized phenomenon warrants careful consideration in subsequent structural optimization.

4.3 Optimization Analysis

In this study, a multi-objective optimization of the proposed structure is performed using the non-dominated sorting genetic algorithm-II (NSGA-II). The optimization process spans 45 generations with a population size of 200 individuals per generation, resulting in the evaluation of 9,000 distinct topological configurations. The objectives are to maximize the overall torque density (T_d) and minimize the torque ripple (T_r), which can be formulated as:

$$T_d = \frac{T_{avg-i} + T_{avg-o}}{V} \tag{6}$$

$$T_r = \max\left(\frac{T_{rip-i}}{T_{avg-i}}, \frac{T_{rip-o}}{T_{avg-o}}\right) \tag{7}$$

where T_{avg-i} and T_{avg-o} are the average torque of the in ner rotor and outer rotor, respectively. V is the electromag netic part volume of the motor. T_{rip-i} and T_{rip-o} are the t orque ripple of inner and outer rotor, respectively. Fig. 8 s hows the Pareto fronts of the last optimization generati on data. The datum line represents the 10% torque rip ple baseline.

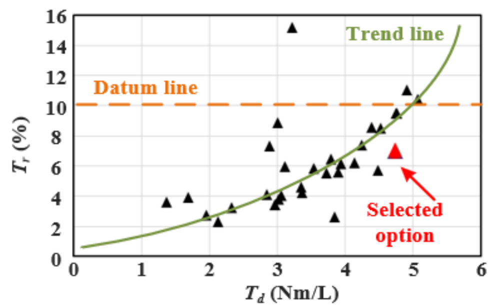

Fig. 8. Pareto fronts of the structure parameters optimization.

Table 2. The optimized structural parameters of proposed topology.

	Optimized Range	Optimized Value
α_{ri}	1°-10°	3.44°
α_{ro}	2°-12°	6.73°
lrt_i	2-10mm	4.84mm
lrt_o	2-10mm	6.12mm
hy_r	2-11mm	4.05mm
hy_s	6-20mm	10.55mm
b_{pm}	2-9mm	3.53mm
bts_i	2-10mm	5.41mm
bts_o	3-12mm	8.23mm
hs_i	4-15mm	12.07mm
hs_o	4-12mm	5.96mm
bs_i	2-9mm	5.6mm
bs_o	3-12mm	10.9mm

Table 2 summarizes the key design parameters and their respective variation ranges used in the optimization process, primarily encompassing rotor teeth, stator slot dimensions, and PM height. The geometric definitions of these parameters within the proposed topology are illustrated in the schematic diagram on Fig. 9.

Further FEM analysis was conducted on the optimized topology, with a detailed performance comparison summarized in Table 3. The results indicate significant enhancements in both back-EMF amplitude and torque output. Specifically, the back-EMF amplitude of winding II has doubled. The T_{avg} of the inner and outer rotors increased by 113% and 35%, respectively, boosting the overall T_d by 54% to 4.59 Nm/L. Regarding T_{rip}, an improvement is observed in the inner rotor while the outer rotor shows a slight increase; nonetheless, the total system ripple remains comparable to the original design and within acceptable limits. Notably, the PM volume was reduced by approximately 40%, demonstrating a superior design that achieves higher output with lower PM usage.

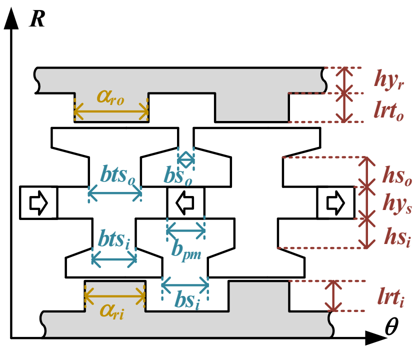

Fig. 9. Annotation diagram for parameters in cylindrical coordinate system.

Table 3. The comparison between optimized and original performance of proposed topology.

	Original	Optimized
Amplitude of winding I back EMF	0.94V/Turn	1.08V/Turn
Amplitude of winding II back EMF	0.33V/Turn	0.65V/Turn
T_{avg-i}	2.2Nm	4.69Nm
T_{avg-o}	6.87Nm	9.27Nm
T_{rip-i}	8.2%	4.3%
T_{rip-o}	4.7%	8.5%
T_d	2.98Nm/L	4.59Nm/L
T_r	8.2%	8.5%
Volume of PMs	115.08mL	71.46mL

5. Conclusion

A novel DR-DFS-PM motor is proposed, merging the advantages of PMSMs and FSPMMs. Featuring FS structures in both rotors and a stator PM design, the motor offers improved robustness and a torque density of 4.59 Nm/L. When coupled with a gearbox for performance amplification, this dual-rotor topology provides a superior alternative for complex high-performance tasks. Notably, the 40% reduction in PM usage achieved through optimization enhances its cost-effectiveness, aligning with the primary economic considerations of modern industrial design.

Acknowledgements

This work was supported by The Hong Kong Polytechnic University under Projects P0056361 and P0052647.

References

[1] K. T. Chau, "Pure electric vehicles," Alternative Fuels and Advanced Vehicle Technologies for Improved Environmental Performance, Woodhead Publishing, pp. 655-684, Mar. 2014.

[2] W. X. Shen, K. T. Chau, C. C. Chan, and E. W. C. Lo, "Neural network based residual capacity indicator for nickel-metal hydride batteries in electric vehicles," IEEE Trans. Veh. Technol., vol. 54, no. 5, pp. 1705-1712, Sep. 2005.

[3] K. T. Chau and C. C. Chan, "Emerging energy-efficient technologies for hybrid electric vehicles," Proceedings of the IEEE, vol. 95, no. 4, pp. 821-835, Apr 2007.

[4] X. Zhang, K. T. Chau and C. C. Chan, "Overview of thermoelectric generation for hybrid vehicles," J. Asian Electr. Veh., vol. 6, no. 2, pp. 1119-1124, Dec. 2008.

[5] C. C. T. Chow, T. Lubin, M.D. Ainslie, C. H. T. Lee, and K. T. Chau, "Analysis and optimization of permanent magnet and DC-excited ironless superconducting synchronous machines for electric aircraft," IEEE Transactions on Transportation Electrification, vol. 11, no. 5, pp. 12596-12607, Oct. 2025.

[6] W. Han, K. T. Chau, C. Jiang, W. Liu, and W.H. Lam, "Design and analysis of quasi-omnidirectional dynamic wireless power transfer for fly-and-charge," IEEE Transactions on Magnetics, vol. 55, no. 7, Jul. 2019, paper no. 8001709, pp. 1-9.

[7] H. Chen, Y. Zuo, K. T. Chau, W. Zhao, and C. H. T. Lee, "Modern electric machines and drives for wind power generation: A review of opportunities and challenges," IET Renew. Power Gener., vol. 15, no. 9, pp. 1864-1887, Jul. 2021.

[8] Z. Dong, M. Jiang, S. Niu and K. T. Chau, "Overview of Permanent Magnet Wind Power Generators," in *IEEE Transactions on Magnetics*, vol. 61, no. 9, pp. 1-11, Sep. 2025.

[9] Y. Du, K. T. Chau, M. Cheng, Y. Fan, W. Zhao, and F. Li, "A linear stator permanent magnet vernier HTS machine for wave energy conversion," IEEE Trans. Appl. Supercond., vol. 22, no. 3, p. 5202505, pp. 1-5, Jun. 2012.

[10] T. W. Ching, K. T. Chau, and W. Li, “Power factor improvement of a linear vernier permanent-magnet machine using auxiliary DC field excitation,” IEEE Trans. Magn., vol. 52, no. 7, p. 8204804, pp. 1-4, Jul. 2016.
[11] L. Jian, K. T. Chau, Y. Gong, C. Yu, and W. Li, “Analytical calculation of magnetic field in surface-inset permanent magnet motors,” IEEE Trans. Magn., vol. 45, no. 10, pp. 4688-4691, Oct. 2009.
[12] Y. Wang, M. Cheng, M. Chen, Y. Du, and K. T. Chau, “Design of high-torque-density double-stator permanent magnet brushless motors,” IET Electr. Power Appl., vol. 5, no. 3, pp. 317-323, Mar. 2011.
[13] X. Li, K. T. Chau, and M. Cheng, “Comparative analysis and experimental verification of an effective permanent-magnet vernier machine,” IEEE Trans. Magn., vol. 51, no. 7, p. 8203009, pp. 1-9, Jul. 2015.
[14] J. Li, K. T. Chau, and W. Li, “Harmonic analysis and comparison of permanent magnet vernier and magnetic-geared machines,” IEEE Trans. Magn., vol. 47, no. 10, pp. 3649-3652, Oct. 2011.
[15] L. Jian, K. T. Chau and J. Z. Jiang, "An Integrated Magnetic-Geared Permanent-Magnet In-Wheel Motor Drive for Electric Vehicles, " IEEE Vehicle Power and Propulsion Conference, pp. 1-6, Sep. 2008.
[16] C. Liu, K.T. Chau and Z. Zhang, “Novel design of double-stator single-rotor magnetic-geared machines” IEEE Trans. Magn., vol. 48, no. 11, pp. 4180-4183, Nov. 2012.
[17] K. T. Chau, Y. B. Li, J. Z. Jiang, and C. Liu, “Design and analysis of a stator-doubly-fed doubly-salient permanent-magnet machine for automotive engines,” IEEE Trans. Magn., vol. 42, no. 10, pp. 3470-3472, Oct. 2006.
[18] C. Liu, K. T. Chau, and W. Li, “Comparison of fault-tolerant operations for permanent-magnet hybrid brushless motor drive,” IEEE Trans. Magn., vol. 45, no. 6, pp. 1378-1381, Jun. 2010.
[19] M. Cheng, F. Yu, K. T. Chau, and W. Hua, “Dynamic performance evaluation of a nine-phase flux-switching permanent magnet motor drive with model predictive control,” IEEE Trans. Ind. Electron., vol. 63, no. 7, pp. 4539-4549, Jul. 2016.
[20] W. Zhao, M. Cheng, K.T. Chau and C.C. Chan, “Control and operation of fault-tolerant flux-switching permanent-magnet motor drive with second harmonic current injection,” IET Electric Power Applications, vol. 6, no. 9, Nov. 2012, pp.707-715.
[21] J. H. Chen, K. T. Chau, S. M. Siu, and C. C. Chan, “Experimental stabilization of chaos in a voltage-mode DC drive system,” IEEE Trans. Circuits Syst. I: Fundam. Theory Appl., vol. 47, no. 7, pp. 1093-1095, Jul. 2000.
[22] C. C. Chan, L. Yan, P. Chen, Z. Wang and K. T. Chau, “Analysis of electromagnetic and thermal fields for induction motors during starting,” IEEE Trans. Energy Convers., vol. 9, no. 1, pp. 53-60, Mar. 1994.
[23] Y. Gao and K. T. Chau, “Hopf bifurcation and chaos in synchronous reluctance motor drives,” IEEE Trans. Energy Convers., vol. 19, no. 2, pp. 296-302, Jun. 2004.
[24] M. Jiang and S. Niu, "Overview of Dual Mechanical Port Machines in Transportation Electrification," in *IEEE Transactions on Transportation Electrification*, vol. 10, no. 3, pp. 4959-4977, Sep. 2024.
[25] M. Jiang, S. Niu and C. Chuen Chan, "A High-Order-Harmonic Compound-Rotor Based Brushless Doubly-Fed Machine for Variable Speed Constant Frequency Wind Power Generation," in *IEEE Journal of Emerging and Selected Topics in Power Electronics*, vol. 13, no. 2, pp. 1492-1502, April 2025.
[26] Z. Dong, M. Jiang and S. Niu, "Novel Radial-Type Permanent Magnet Generators with Mechanical Flux-Weakening Design for VSCAV Control in Wind Power Generation," *IEEE International Conference on Electrical Energy Conversion Systems and Control*, 2024, pp. 62-66.
[27] Z. Liang, X. Ren, D. Li, R. Qu and X. Han, "Analysis of a Spoke-Array Brushless Dual-Electrical-Port Dual-Mechanical-Port Machine with Reluctance Rotor," in *IEEE Transactions on Industrial Electronics*, vol. 68, no. 4, pp. 2999-3011, April 2021
[28] M. Jiang and S. Niu, "A High-Order Harmonic Compound Rotor Based Brushless Dual-Electrical-Port Dual-Mechanical-Port Machine," in *IEEE Transactions on Industrial Electronics*, vol. 71, no. 6, pp. 5463-5473, June 2024.
[29] F. Ni, Z. Li, S. Niu and C. Liu, "Complementary Series Magnetic Circuit-Based Stator-Yokeless Dual-Rotor PM Vernier Reluctance Machine for In-Wheel Propulsion," in *IEEE Transactions on Transportation Electrification*, vol. 11, no. 1, pp. 4551-4560, Feb. 2025.
[30] M. Jiang, W. Fu and S. Niu, "Design and Analysis of a Novel Dual-Airgap Dual Permanent Magnet Vernier Machine," in *IEEE Access*, vol. 9, pp. 57188-57197, 2021.
[31] H. Zhao, C. Liu, Z. Dong, R. Huang and X. Li, "De sign and Optimization of a Magnetic-Geared Direct-Drive Machine With V-Shaped Permanent Magnets f or Ship Propulsion," in *IEEE Transactions on Trans portation Electrification*, vol. 8, no. 2, pp. 1619-163 3, June 2022.
[32] Z. Wang, J. Yang, S. Dai, Y. Feng and S. Huang, "Novel Dual-Rotor Single-Stator Coreless Permanent Magnet Machine with Dual-Flywheel," in *IEEE Transactions on Magnetics*, vol. 58, no. 8, pp. 1-6, Aug. 2022, Art no. 8106506.
[33] L. Dai, S. Niu, Z. Lyu, X. Huang and K. T. Chau, "Challenges and Opportunities in Electric Propulsion Systems for Low-Altitude eVTOL Aircraft," in *IEEE Transactions on Power Electronics*.
[34] S. Niu, S. Wang and X. Zhao, "Overview of Stator Slot-Opening Permanent Magnet Machines," in *IEEE Transactions on Transportation Electrification*, vol. 9, no. 1, pp. 782-804, March 2023.
[35] Y. Du, F. Xiao, W. Hua, X. Zhu, M. Cheng, L. Quan, and K. T. Chau, "Comparison of Flux-Switching PM Motors with Different Winding Configurations Using Magnetic Gearing Principle," in *IEEE Transactions on Magnetics*, vol. 52, no. 5, p. 8201908, May 2016.

[36] Y. Bi, W. Fu, S. Niu, X. Zhao, J. Huang and Z. Qiao, "Torque Enhancement of a Dual PM Flux-Switching Machine with Improved Multiple High-Order Working Harmonics," in *IEEE Transactions on Transportation Electrification*, vol. 10, no. 2, pp. 2830-2843, June 2024.
[37] C. Chen, X. Ren, D. Li, R. Qu, K. Liu and T. Zou, "Torque Performance Enhancement of Flux-Switching Permanent Magnet Machines with Dual Sets of Magnet Arrangements," in *IEEE Transactions on Transportation Electrification*, vol. 7, no. 4, pp. 2623-2634, Dec. 2021.
[38] W. Zhao, M. Cheng, K. T. Chau, W. Hua, H. Jia, J. Ji and W. Li, "Stator Flux-Oriented Fault-Tolerant Control of Flux-Switching Permanent Magnet Motors," in *IEEE Transactions on Magnetics*, vol. 47, no. 10, pp. 4191-4194. Oct. 2011.
[39] Y. Bi, W. Fu, S. Niu, X. Zhao and J. Huang, "Design of a Dual-Set Permanent Magnet Flux-Switching Machine with Enhanced Torque Density and Fault-Tolerance Capability," in *IEEE Transactions on Transportation Electrification*, vol. 10, no. 4, pp. 9096-9108, Dec. 2024.
[40] L. Cao, K. T. Chau, C. H. T. Lee and H. Wang, "A Double-Rotor Flux-Switching Permanent-Magnet Motor for Electric Vehicles with Magnetic Differential," in *IEEE Transactions on Industrial Electronics*, vol. 68, no. 2, pp. 1004-1015, Feb. 2021.
[41] Z. Wang, J. Yang, S. Dai, Y. Feng and S. Huang, "Novel Dual-Rotor Single-Stator Coreless Permanent Magnet Machine with Dual-Flywheel," in I*EEE Transactions on Magnetics*, vol. 58, no. 8, pp. 1-6, Aug. 2022.
[42] W. Zhao, T. A. Lipo and B. -I. Kwon, "A Novel Dual-Rotor, Axial Field, Fault Tolerant Flux-Switching Permanent Magnet Machine with High-Torque Performance," in IEEE Transactions on Magnetics, vol. 51, no. 11, pp. 1-4, Nov. 2015.
[43] Z. Dong, M. Jiang and Z. Huang, "Guideline of Integrated Winding for Dual Mechanical-Port Machines," *2025 IEEE 20th Conference on Industrial Electronics and Applications (ICIEA)*, Yantai, China, 2025, pp. 1-6.
[44] H. Chen, A. M. EL-Refaie, Y. Zuo, S. Cai, S. Xie and C. H. T. Lee, "Evaluation of a Contra-Rotating Flux-Modulated Machine Featured with Dual Flux-Modulation for Wind Power Generation," in *IEEE Transactions on Industrial Electronics*, vol. 69, no. 9, pp. 8770-8781, Sept. 2022.

Zixu Dong
Zixu Dong received the B.Eng. degree in electrical engineering and automation from Taiyuan University of Technology, Taiyuan, China in 2021. Subsequently, he obtained the M.Sc. degrees in electrical engineering from The Hong Kong Polytechnic University, Hong Kong, China, in 2025. He is currently working toward the Ph.D. degree in the Department of Electrical and Electronic Engineering, The Hong Kong Polytechnic University, Hong Kong, China. His research interests include design, optimization, and control of electric machines, electric vehicles, and power generation.

Mingyuan Jiang
Mingyuan Jiang received the B.Eng. degree in Electrical Engineering and Automation from Shanghai Maritime University, Shanghai, China, in 2020. He subsequently obtained his M.Sc. and Ph.D. degrees in Electrical Engineering from The Hong Kong Polytechnic University, Hong Kong, China, in 2021 and 2024, respectively.
He is currently a Research Assistant Professor in the Department of Electrical and Electronic Engineering and a member of the Research Centre for Electric Vehicles (RCEV) at The Hong Kong Polytechnic University. He is currently the Guest Editor and long-term reviewer for several well-known SCI journals. His primary research interests include the design, optimization, and control of electric machines, transportation electrification, robotics, and power generation systems.

Zhang Zhang
Zhang Zhang received the B.Eng. degree in automation from the University of South China, Hengyang, China, in 2022, and the M.Eng. degree in control engineering from Shenzhen University, Shenzhen, China, in 2025. He is currently working toward the Ph.D. degree in electrical engineering with Department of Electrical and Electronic Engineering, The Hong Kong Polytechnic University, Hong Kong, China. His research interests include servo motor drives, control theory, and intelligent systems.

Zhouyang Zhang
Zhouyang Zhang received the B.Eng. degree in Robotics Engineering from Wuhan University of Technology, Wuhan, China, in 2025. He is currently working toward the M.Phil. degree in electrical engineering with Department of Electrical and Electronic Engineering, The Hong Kong Polytechnic University, Hong Kong, China. His research interests include electric vehicles and machine design.

Shuangxia Niu
Shuangxia Niu received the B.Sc. and M.Sc. degrees in electrical engineering from Tianjin University, Tianjin, China, in 2002 and 2005, respectively, and the Ph.D. degree in electrical engineering from the University of Hong Kong, Hong Kong, China, in 2009.
She is currently a Professor with the Department of Electrical and Electronic Engineering, The Hong Kong Polytechnic University, Hong Kong. She has authored or coauthored more than 100 papers in leading journals. er research interests include the electric vehicle technologies, renewable energy systems, machines and drives, power electronics technology, applied electromagnetic, numerical method, and optimization.

K.T. Chau
K.T. Chau received the B.Sc. (Eng.), M.Phil., and Ph.D. degrees in electrical and electronic engineering from The University of Hong Kong, Hong Kong, China, in 1988, 1991, and 1993, respectively.
He serves as a Chair Professor in electrical energy engineering with the Research Centre for Electric Vehicles and Department of Electrical and Electronic Engineering, The Hong Kong Polytechnic University, Hong Kong. His research interests include electric and hybrid vehicles, power electronics and drives, and renewable energies. He is the author of nine books and more than 350 journal papers.
Prof. Chau is a fellow of the Institution of Engineering and Technology (IET), U.K., and the Hong Kong Institution of Engineers. He is a Chartered Engineer. He was the recipient of the Changjiang Chair Professorship from the Ministry of Education, China, and the Environmental Excellence in Transportation Award for Education, Training, and Public Awareness from the Society of Automotive Engineers International.

C.C. Chan
C.C. Chan was born in 1937. He received the B.S. degree from China University of Mining and Technology, Xuzhou, China, in 1957, the M.S. degree from Tsinghua University, Beijing, China, in 1959, and the Ph.D. degree from the University of Hong Kong, Hong Kong, China, in 1982, all in electrical engineering. He is currently a Distinguished Chair Professor of electric vehicles and smart energy with the Department of Electrical and Electronic Engineering, Hong Kong Polytechnic University, Hong Kong. He has more than 50 years of teaching and research experience and proposes engineering philosophy, engineering, and education innovation, which laid the foundation of modern electric vehicles theory and electric vehicles electric drive theory. He has authored more than 300 papers and 11 monographs. Prof. Chan is a member of the Chinese Academy of Engineering and the Ukrainian Academy of Engineering Sciences, a fellow of the Royal Academy of Engineering U.K., and an Honorary Fellow of the Hungarian Academy of Engineering. He is a Senior IET Fellow and the Former President of the Hong Kong Institution of Engineers. He was a recipient of the Toastmasters Medal by the Institution of Electrical Engineers (IEE) in 2000, Father of Asian Electric Vehicles by Magazine Global View in 2003, Environmental Excellence in Transportation Award by the Society of Automotive Engineers (SAE) in 2007, Gold Medal of Hong Kong Institution of Engineers in 2010, World Federation of Engineering (WFEO) Medal for Engineering Excellence in 2013, Prince Philip Medal of U.K. Royal Academy of Engineering in 2014, and IEEE Transportation Technologies Award by IEEE in 2018.